Helical Arrays of CdS Nanoparticles Tracing on a Functionalized Chiral Template of Glycolipid Nanotubes

Yong Zhou, Qingmin Ji, Mitsutoshi Masuda, Shoko Kamiya, and Toshimi Shimizu*

CREST, Japan Science and Technology Agency (JST), Tsukuba Central 4, 1-1-1 Higashi, Tsukuba, Ibaraki 305-8562, Japan, and Nanoarchitectonics Research Center (NARC), National Institute of Advanced Industrial Science and Technology (AIST), Tsukuba Central 5, 1-1-1 Higashi, Tsukuba, Ibaraki 305-8565, Japan

Received August 26, 2005. Revised Manuscript Received November 4, 2005

We have illustrated that the dense helical arrays of CdS nanoparticles, which are aligned one-by-one and side-by-side, form on the self-assembled nanotube template from the binary components, glycolipid, *N*-(11-*cis*-octadecenoyl)-*β*-D-glucopyranosylamine (**1**) and aminophenyl-*β*-D-glucopyranoside (**2**) as an additive. The present formation mechanism greatly differs from preceding examples that utilize residual helical marks on the surfaces of lipid nanotubes and nanoribbons or organic templates with a helical morphology. In this work, we functionalized the glycolipid nanotube of **1** by incorporation of **2** through self-assembly. This functionalization process enabled us to create active binding sites, which trace the chiral molecular packing of the nanotube. Consequently, the helical nucleation and growth of the CdS nanoparticles took place on the template surfaces. The helical arrangement of the CdS nanoparticles was characterized by field-emission scanning electron microscopy (FE-SEM) and scanning transmission electron microscopy (STEM). The phase analysis and optical properties of the helical CdS nanoparticle were also discussed.

Introduction

Realization of technologically useful nanomaterials with tunable electronic, magnetic, and optical properties depends on the quality of nanocrystals (e.g., size and shape), their surface properties, and spatial orientation and arrangement.[1] In recent years, benefiting from the specific properties such as precise molecular recognition, there has been much interest in using biological molecules to modulate the growth of a large variety of inorganic nanomaterials including metal, semiconductor, and magnetic particles.[2−10] In particular, the use of biomolecular tubules or fibers as scaffolds allowed one to manipulate the size,[11] shape,[12] and even packing density[13] of nanoparticles. Nevertheless, the control of spatial orientation and arrangement of each nanoparticle on such biomolecular substrates has been challengeable to achieve. In particular, helical inorganic materials have specific applications as asymmetric reaction catalysts, helical sensors, and optical materials.[2] Significant examples using biomolecules as templates involve the formation of helical arrays of nanoparticles on lipid nanotubes[14] and nanoribbons.[15,16] However, most of them mainly focuses on metal (e.g., Au, Pd, and Cu) and SiO_2. The helical patterns of semiconductor nanoparticles are rarely reported.[16b] Recently, chemical modification of a biomolecular 1-D scaffold with functional molecules has emerged as an attractive and practicable way to rationally tailor the properties of the scaffolds. It can create preferential binding sites to nucleate and organize nanoparticles.[17,18]

In this paper, we describe the formation of the helical arrays of CdS nanoparticles on a functionalized lipid nanotube (FLNT) template, which self-assembled from a structurally optimized glycolipid, *N*-(11-*cis*-octadecenoyl)-*β*-D-

* To whom correspondence should be addressed. E-mail: tshmz-shimizu@aist.go jp. Fax: +81-29-861-4545.
† CREST, JST.
‡ NARC, AIST.

(1) Zhou, Y. *Curr. Nanosci.* **2005**, *1*, 35.
(2) Shimizu, T.; Masuda, M.; Minamikawa, H. *Chem. Rev.* **2005**, *105*, 1401.
(3) (a) Cölfen, H.; Mann, S. *Angew. Chem., Int. Ed.* **2003**, *42*, 2350. (b) Yu, S. H.; Cölfen, H. *J. Mater. Chem.* **2004**, *14*, 2124. (c) Yu, S. H.; Cölfen, H.; Tauer, K.; Antonietti, M. *Nat. Mater.* **2005**, *4*, 51.
(4) Braun, E.; Eichen, Y.; Sivan, U.; Ben-Yoseph, G. *Nature* **1998**, *391*, 775.
(5) Hutchison, J. E.; Warner, M. G. *Nat. Mater.* **2003**, *2*, 272.
(6) Douglas, D. A.; Mann, S. *Nature* **1993**, *364*, 430.
(7) (a) Yan, H.; Park, S. H.; Finkelstein, G.; Reif, J. H.; LaBean, T. H. *Science* **2003**, *301*, 1882. (b) Li, H.; Park, S. H.; Reif, J. H.; Labean, T. H.; Yan, H. *J. Am. Chem. Soc.* **2004**, *126*, 418.
(8) Reches, M.; Gazit, E. *Science* **2003**, *300*, 625.
(9) (a) Yang, B.; Kamiya, S.; Shimizu, Y.; Koshizaki, N.; Shimizu, T. *Chem. Mater.* **2004**, *14*, 2826. (b) Yang, B.; Kamiya, S.; Yoshida, K.; Shimizu, T. *Chem. Commun.* **2004**, 500. (c) Yui, H.; Shimizu, Y.; Kamiya, S.; Yamashita, I.; Masuda, M.; Ito, K.; Shimizu, T. *Chem. Lett.* **2005**, *34*, 232.
(10) Le, J. D.; Pinto, Y.; Seeman, N. C.; Musier-Forsyth, K.; Taton, T. A.; Kiehl, R. A. *Nano Lett.* **2004**, *3*, 2343.
(11) Banerjee, I. A.; Yu, L.; Matsui, H. *Proc. Natl. Acad. Sci. U.S.A.* **2003**, *100*, 14678.
(12) Yu, L.; Banerjee, I. A.; Matsui, H. *J. Am. Chem. Soc.* **2003**, *125*, 14837.
(13) Djalali, R.; Chen, Y.; Matsui, H. *J. Am. Chem. Soc.* **2003**, *125*, 5873.
(14) (a) Burkett, S. L.; Mann, S. *Chem. Commun.* **1996**, 321. (b) Lvov, Y. M.; Price, R. R.; Selinger, J. V.; Singh, A.; Spector, M. S.; Schnur, J. M. *Langmuir* **2000**, *16*, 5932. (c) Price, R. R.; Dressick, W. J.; Singh, A. *J. Am. Chem. Soc.* **2003**, *125*, 11259.
(15) (a) van Bommel, K. J. C.; Friggeri, A.; Shinkai, S. *Angew. Chem., Int. Ed.* **2003**, *42*, 980. (b) Jung, J. H.; Yoshida, K.; Shimizu, T. *Langmuir* **2002**, *18*, 8724. (c) Jung, J. H.; Rim, J. A.; Lee, S. J.; Lee, S. S. *Chem. Commun.* **2005**, 468.
(16) (a) Hartgerink, J. D.; Beniash, E.; Stupp, S. I. *Science* **2001**, *294*, 1684. (b) Sone, E. D.; Zubarev, E. R.; Stupp, S. I. *Angew. Chem., Int. Ed.* **2002**, *41*, 1706.
(17) Li, L. S.; Stupp, S. I. *Angew. Chem., Int. Ed.* **2005**, *44*, 1833.
(18) Mao, C.; Solis, D. J.; Reiss, B. D.; Kottmann, S. T.; Sweeney, R. Y.; Hayhurst, A. H.; Georgiou, G.; Iverson, B.; Belcher, A. M. *Science* **2004**, *303*, 213.

10.1021/cm051928z CCC: $33.50
Published on Web 12/21/2005

glucopyranosylamine (**1**)[19] and aminophenyl-β-D-glucopyranoside (**2**).

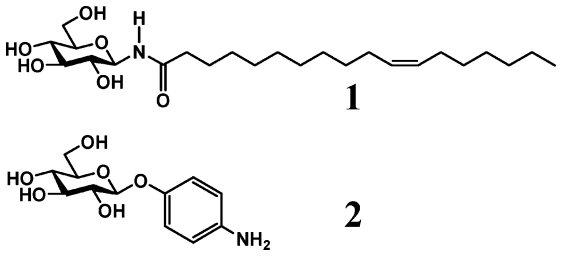

Experimental Section

The synthesis of the nanotube **1** functionalized with **2** was carried out in a way similar to that of pure nanotube **1** as reported previously.[19] Typically, **1** (1.0 mg, 2.34 μmol) and **2** (0.60 mg, 2.34 μmol) were dissolved in 1 mL of methanol in a round-bottom flask, and then the solution was evaporated at 40 °C with a rotary vacuum evaporator for 30 min, followed by further drying in a vacuum for 1 h at room temperature to remove the residual methanol completely. To the obtained lipid thin film on the glass wall was added 20 mL of Milli-Q water (conductivity < 18 MΩ·cm) in the flask. The solution was refluxed at 120 °C for 2 h, then cooled to 60 °C slowly, and kept there for 12 h. Finally, the solution was allowed to cool to room temperature. Thus, we obtained a transparent suspension of the nanotube **1** functionalized with **2**. The FT-IR spectra revealed that the observed molar ratio of **2** to **1** is approximately 16% in the FLNT by comparison of the peak intensity of the amide II (−NH−) band of **1** before and after doping. In a typical procedure for the preparation of ordered CdS arrays on the FLNTs, $Cd(NO_3)_2$ (0.1 M, 1 mL) and thioacetamide (TAA) (0.1 M, 1 mL) as a source solution of S^{2-} were added dropwise into 8 mL of the aqueous FLNT suspension with stirring. The reaction mixture was continuously stirred for 1 day to complete the reaction. Slow release of S^{2-} from TAA resulted in mild deposition of CdS nanoparticles on the nanotube in the suspension. The obtained product was filtered and washed with Milli-Q water several times for further characterization. The field-emission scanning electron microscopy (FE-SEM) and scanning transmission electron microscopy (STEM) measurement of the samples were carried out with an Hitachi S-4800. X-ray powder diffraction patterns (XRD) of the product were obtained on a Japan Rigaku DMax-γA rotation anode X-ray diffractomer equipped with graphite monochromatized Cu Kα radiation (λ = 1.54178 Å). The UV−vis spectrum was recorded on an Hitachi U-3300 at room temperature. The photoluminescence (PL) spectrum was performed on an Hitachi F-4500 fluorescence spectrophotometer at room temperature.

Results and Discussion

Figure 1 shows the FE-SEM and STEM images of the FLNT, indicating that the nanotube structures with a well-defined cylindrical hollow are intact as compared to the pure LNT from **1**.[19] The FLNT with a smooth surface possesses a cylindrical hollow as a core. The outer diameters and wall thickness of the FLNT are 150−400 and 30−40 nm, respectively. The lengths range from several micrometers up to tens of micrometers.

Figures 2a−2c show the time-resolved high-resolution FE-SEM images that trace the formation of helical arrays of

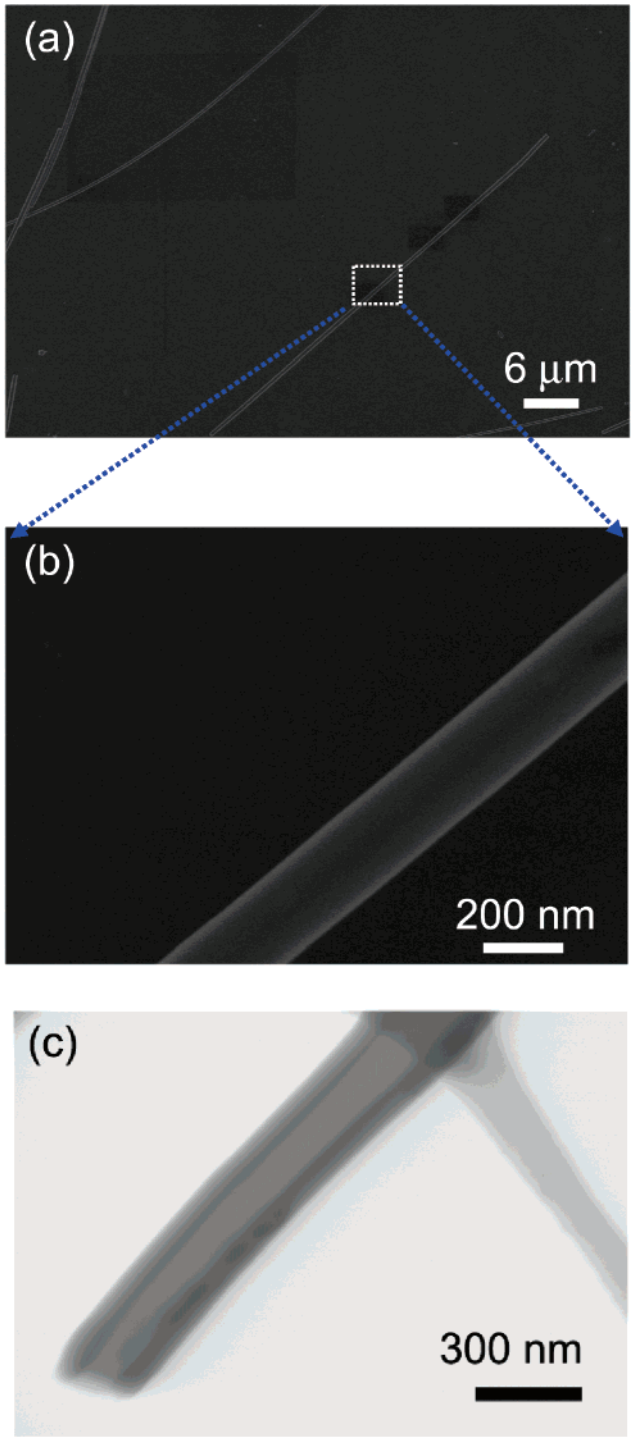

Figure 1. (a) FE-SEM image of the FLNT obtained by binary self-assembly of **1** and **2.** (b) A magnified FE-SEM image of the selected area. (c) A STEM image of the FLNT.

CdS nanoparticles on the FLNT surface. Figure 2a revealed that at the initial stage CdS selectively nucleated and grew into nanoparticles on the FLNT. These nanoparticles connected one-by-one in a 1-D pattern, twinning the curved surface of the FLNT scaffold, as marked by solid arrows. The existence of a gap between the sections (shown as dot arrows) indicates that there are many nucleation sites in the 1-D growth track along the FLNT. With reaction time, the discontinuous connection of the nanoparticles evolved into chain- and nanowire-like architectures along the scaffold (Figure 2b). (Three more images are available in the

(19) Kamiya, S.; Minamikawa, H.; Jung, J. H.; Yang, B.; Masuda, M.; Shimizu, T. *Langmuir* **2005**, *21*, 743.

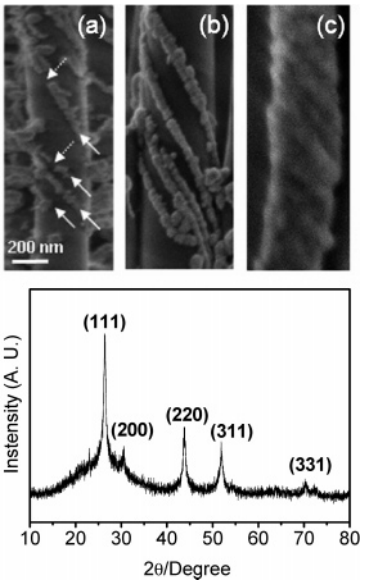

Figure 2. Time-resolved high-resolution FE-SEM images that show the formation of the helical array of CdS nanoparticles on the FLNT surface for (a) 3 h, (b) 5 h, and (c) 1 day. XRD pattern of the obtained helical arrays of CdS nanoparticles on the FLNT surfaces (bottom).

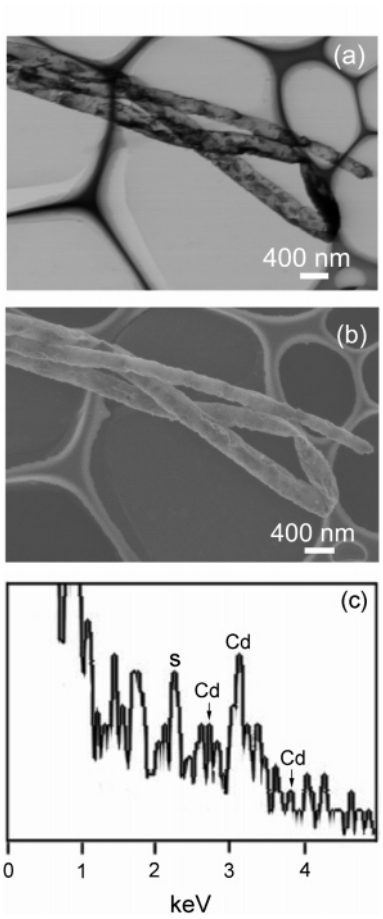

Figure 3. (a) STEM image, (b) FE-SEM image and (c) EDX spectrum for the CdS nanotubes obtained by calcination of the CdS-coated FLNT nanocomposite at 350 °C for 7 h.

Supporting Information.) These nanowires and chains arrange almost in a parallel fashion to one another with tilting by approximately 45° with respect to the long axis of the FLNT. After 1 day of incubation, the helical array of the CdS nanoparticles on the FLNT formed (Figure 2c). The XRD

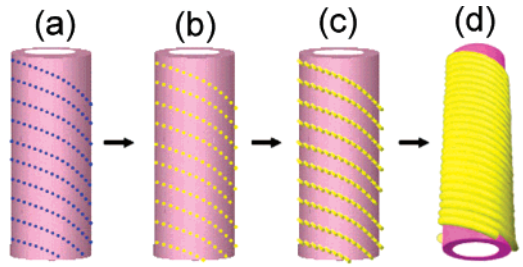

Figure 4. Illustration of the formation mechanism for the helical arrays of CdS nanoparticles on the FLNT surfaces.

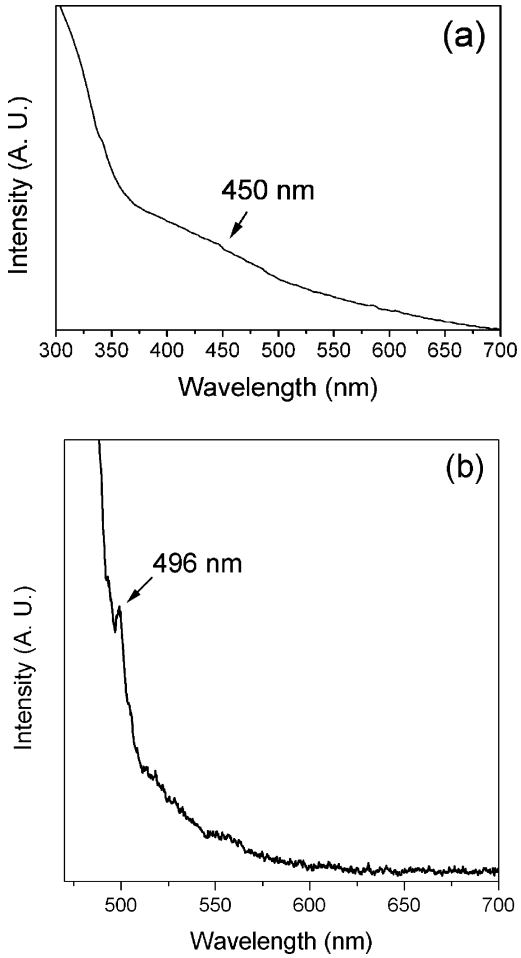

Figure 5. (a) UV−vis absorption and (b) photoluminescence spectra of the CdS nanoparticle nucleated on the FLNT.

pattern in Figure 2 (bottom) demonstrated that the formed CdS nanoparticle is associated with a face-centered-cubic (fcc) phase of zinc blende structure. The above results indicate that the FLNT can act as an efficient template for ordered deposition and preferential growth of the inorganic nanoparticles. To remove the FLNT as an outer organic shell, we calcined the FLNT nanocomposite coated with CdS nanoparticles at 350 °C for 7 h, which is below the melting point of CdS. Consequently, the CdS nanotubes with a hollow were easily obtainable. Figures 3a and 3b show the STEM and corresponding FE-SEM images of the CdS nanotube, respectively. The EDX spectrum of the CdS nanotube in Figure 3c revealed the exact elemental composition of Cd and S.

The present formation mechanism resulting in the helical arrays of CdS nanoparticles on the FLNT differs from the

precedents that utilize either residual helical marks on the surfaces of lipid nanotubes and nanoribbons or organic templates with a helical morphology.[14−18] Our LNT has no helical marks on the outer surfaces.[19] When employing the pure LNT as a template under identical experiment conditions, we found that most of the generated CdS particles aggregate in solutions with only a few randomly depositing on the surface of the LNT. This finding clearly shows that the incorporation of **2** as an additive plays a crucial role in nucleating and guiding the preferential growth of the CdS nanocrystals on the FLNT.[20] Based on the theoretical model for chiral self-assembly of lipid tubules proposed by Helfrich and Prost,[21] we can deduce that the nanotube structure from **1** has the molecular tilt optimally oriented at an angle of 45°. Thus, it is expected that **2** is also distributed in a helical fashion within the LNT membrane, as indicated with the dot curves in Figure 4a. As a result, Cd^{2+} will helically nucleate on the surface of the FLNT through preferential affinity of Cd^{2+} to the amino group of **2**. Interaction with S^{2-}, slowly released by decomposition of TAA, allows the heterogeneous nucleation of CdS along the surface of the FLNT (Figure 4b). Increase in the incubation time promoted the growth of the nuclei into nanoparticles (Figure 4c) and eventually the formation of chain- or wirelike architecture (Figure 4d) helically twinning the FLNT. The left-handed helical sense of the CdS chains on the FLNT suggests the identical helical sense of the chiral molecular packing.

The CdS nanoparticle nucleated on the FLNT shows a broad UV−vis absorption shoulder at around 450 nm as shown in Figure 5a, blue-shifted from 515 nm for bulk CdS.[22] Under photoluminescent excitation at 470 nm, the CdS nanoparticle emits blue light at 496 nm in Figure 5b, also blue-shifted compared with bulk CdS (600−650 nm). These optical features indicate the quantum-confined effects of the CdS nanoparticles on the FLNT.[22]

Conclusions

The helical arrays of the CdS nanoparticles have been fabricated on the FLNT by incorporation of functional molecules. The ordered alignment of the CdS nanoparticles on the nanoscale substrate is applicable in optical and electronic nanodevices due to their unique properties. The present process typically represents a novel step to artificially control the crystal orientation and morphology on bio-inspired substrates.

Supporting Information Available: High-resolution FE-SEM images that show the formation of the helical array of CdS nanoparticles on the FLNT surface. This material is available free of charge via the Internet at http://pubs.acs.org.

CM051928Z

(20) (a) Jung, J. H.; Shinkai, S.; Shimizu, T. *Chem. Rec.* **2003**, *3*, 212. (b) Jung, J. H.; Yoshida, K.; Shimizu, T. *Langmuir* **2002**, *18*, 8724. (c) Ji, Q.; Iwaura, R.; Kogiso, M.; Jung, J. H.; Yoshida, K.; Shimizu, T. *Chem. Mater.* **2004**, *16*, 250.

(21) Helfrich, W.; Prost, J. *Phys. Rev. A* **1988**, *38*, 3065.

(22) Henglein, A. *Chem. Rev.* **1989**, *89*, 1861.